

Inventory of Supplemental Information

Supplemental Figures

Figure S1, related to Figure 1.

Figure S2, related to Figure 2.

Figure S3, related to Figure 4.

Supplemental Tables

Table S1, related to Figure 1.

Table S2, related to Figures 2-4.

Supplemental Experimental Procedures

Supplemental References

Supplemental Figures

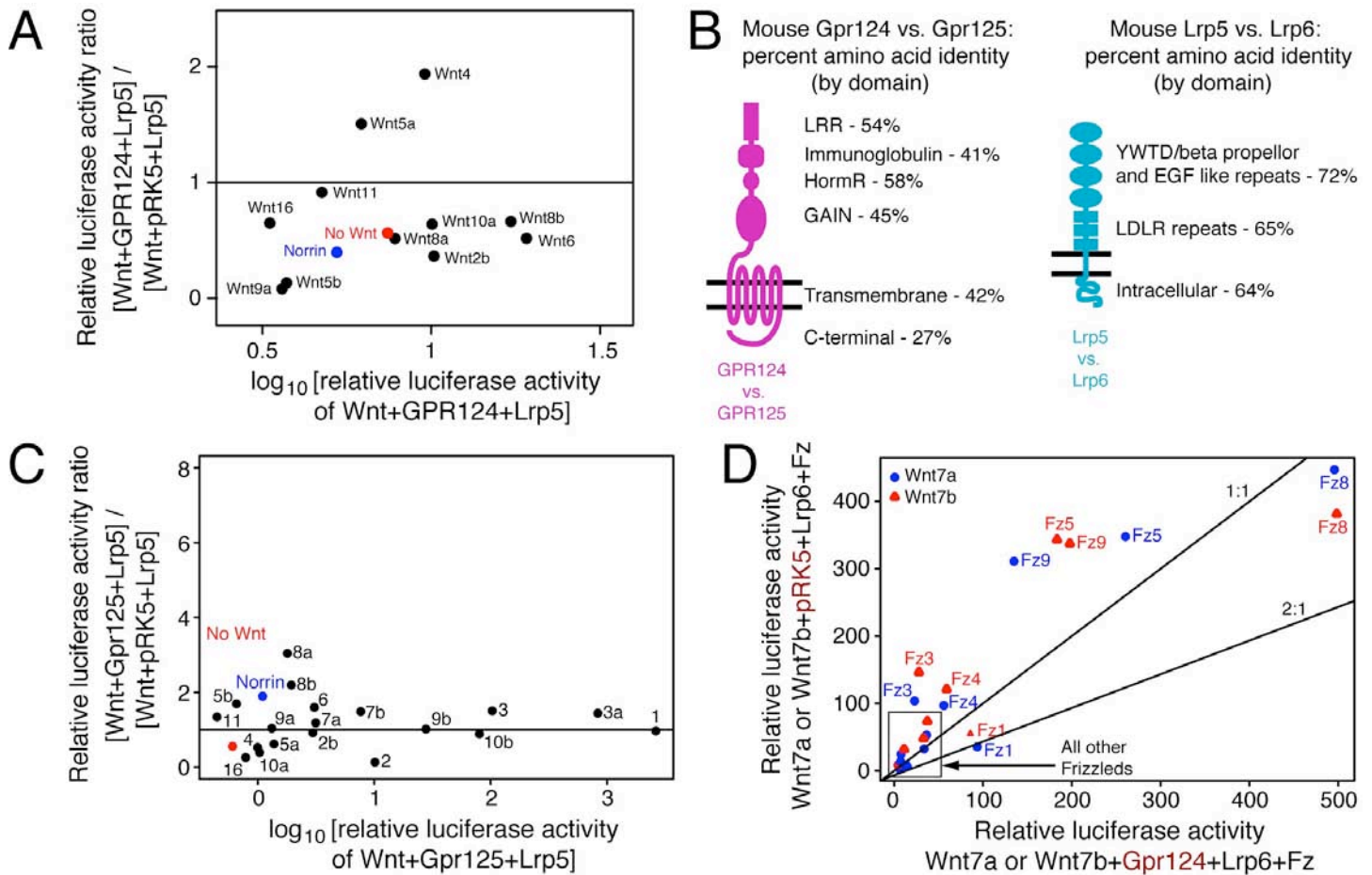


Figure S1, Related to Figure 1. Luciferase activity in STF cells in response to Gpr, Fz, Lrp, and Wnt transfection.

(A) Ratio of luciferase activity induced by Wnt+Gpr124+Lrp5 compared to Wnt+ vector (pRK5)+Lrp5 plotted against luciferase activity induced by Wnt+Gpr124+Lrp5. This panel is an enlargement of the lower left quadrant of Figure 1A, showing the subset of ligands that produced relatively low luciferase activities in STF cells.

(B) Amino acid identities of murine Gpr124 vs. Gpr125 and Lrp5 vs. Lrp6, shown for each domain.

(C) Gpr125 and Lrp5 tested with 19 Wnts and Norrin. Ratio of luciferase activity induced by Wnt+Gpr125+Lrp5 compared to Wnt+vector (pRK5)+Lrp5 plotted against luciferase activity induced by Wnt+Gpr125+Lrp5. Wnt8a and Wnt8b show a small enhancement of activity.

(D) Lrp6 shows little or no synergy with Gpr124. The plot shows the relative luciferase activity of Wnt7a+Lrp6+Fz or Wnt7b+Lrp6+Fz with vector (pRK5) vs. Gpr124. Among the ten mouse Frizzleds, six have activity substantially above background, but only Fz1 shows an enhancement of signaling with Gpr124+Lrp6 (~2-fold).

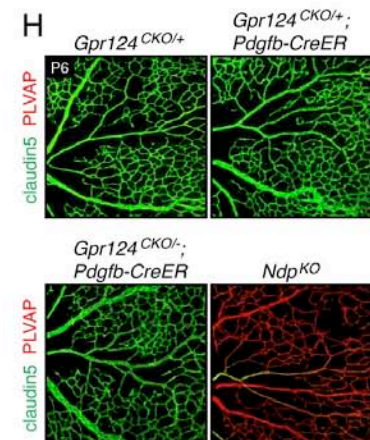
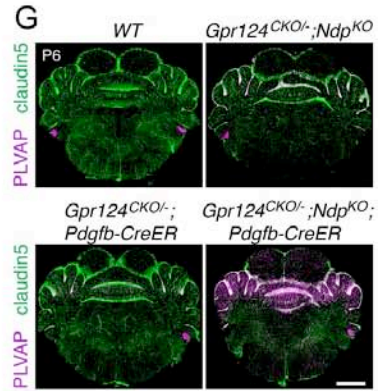
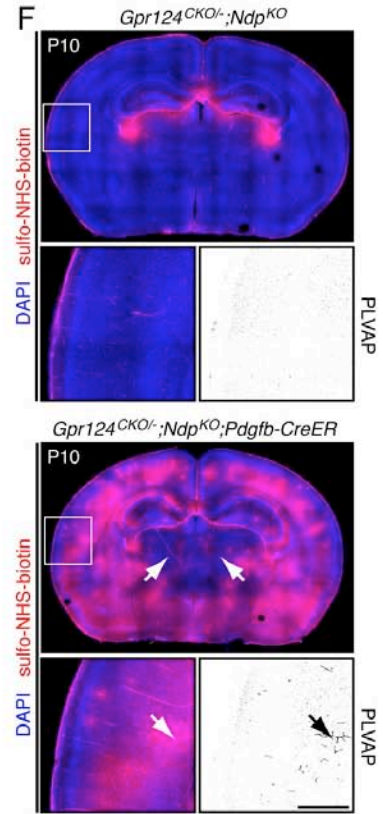
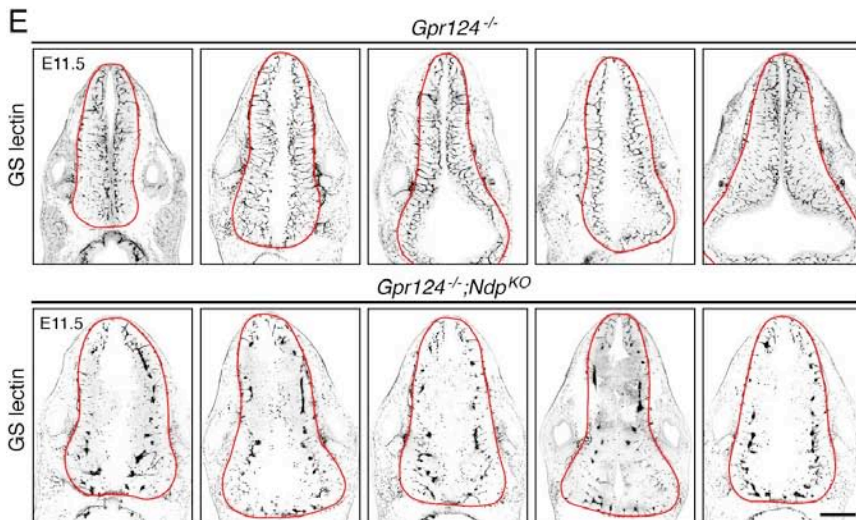
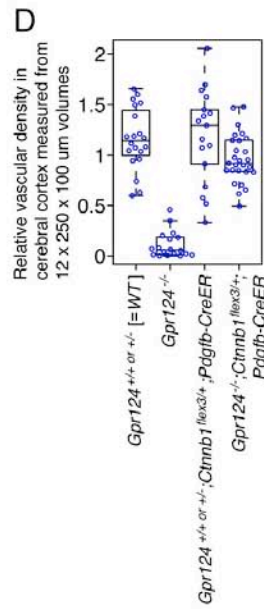
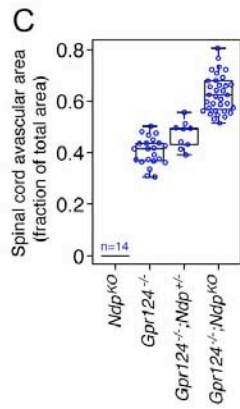
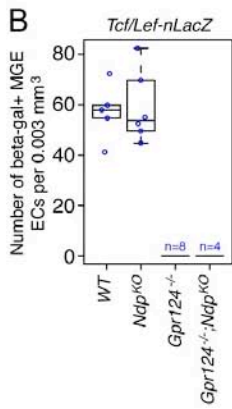
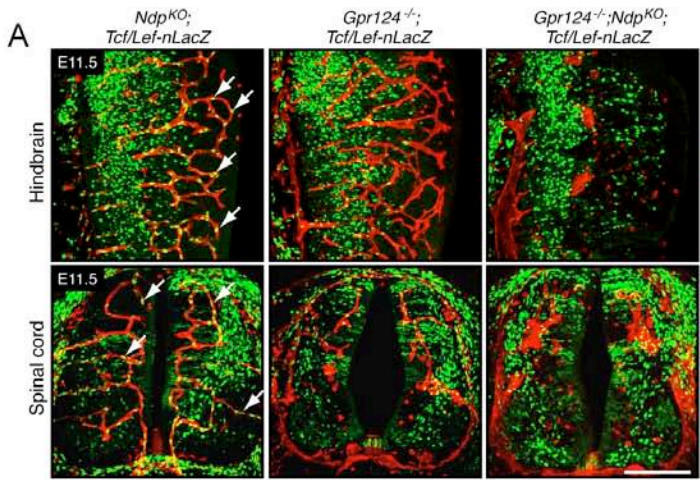


Figure S2, Related to Figure 2. Genetic interaction between *Gpr124* and *Ndp* in CNS angiogenesis and BBB postnatal BBB maintenance.

(A) Canonical Wnt signaling in the hindbrain and spinal cord vasculature visualized with the *Tcf/Lef-nLacZ* reporter. Z-stacked images of E11.5 hindbrain and spinal cord show numerous beta-galactosidase+ nuclei, most of which are in the CNS parenchyma. Among CNS vascular ECs, there is a greater density of beta-galactosidase+ nuclei in the *Ndp^{KO};Tcf/Lef-nLacZ* samples and a lower density of beta-galactosidase+ nuclei in the *Gpr124^{-/-};Tcf/Lef-nLacZ* samples. In Z-stacked images, nuclei of ECs that are part of well-formed blood vessels can generally be distinguished from closely apposed nuclei in neuroepithelial cells because the EC nuclei are typically elongated in the direction of the long axis of the blood vessel. We note that *Gpr124^{-/-};Ndp^{KO};Tcf/Lef-nLacZ* ECs are not well organized and it is therefore difficult to determine in a Z-stacked image whether beta-galactosidase+ nuclei superimposed on the GS lectin signal are vascular or neural. Analysis of single Z-plane images (Figure 2C) suggests that few if any are vascular. Scale bar: 200 μ m.

(B-D) Scatter plots from Figures 2A, 2B, and 4G are reproduced here as panels B, C, and D, respectively, with the individual data points shown. In panel B, the *Gpr124^{-/-}* and *Gpr124^{-/-};Ndp^{KO}* genotypes were represented by 8 and 4 sections, respectively, and have a mean of zero beta-gal+ ECs per section in the MGE. In panel B, the *Ndp^{KO}* genotype is represented by 14 sections and has a mean avascular area of zero μ m² (as described in the Figure 2 legend).

(E) Massive reduction in *Gpr124^{-/-};Ndp^{KO}* hindbrain vascularization at E11.5. GS lectin-stained hindbrain sections from five *Gpr124^{-/-}* embryos and five *Gpr124^{-/-};Ndp^{KO}* embryos. The *Gpr124^{-/-}* embryos show normal or nearly normal vascularization, whereas the *Gpr124^{-/-};Ndp^{KO}* embryos show severely retarded vascularization with glomeruloid body formation throughout the ventral 90% of the hindbrain. These data confirm the phenotypes shown in Figure 2E. Red lines demarcate the borders of the neuroepithelium. Scale bar: 500 μ m.

(F,G) Postnatal redundancy of *Gpr124* and *Ndp* in maintaining the BBB state. In (F) Sulfo-NHS-biotin perfusion to monitor BBB integrity at P10 in *Gpr124^{CKO/-};Ndp^{KO};Pdgfb-CreER* mice is shown in coronal sections at the level of the anterior hippocampus. In this experiment, residual CreER activity in the absence of tamoxifen or 4HT exposure provided sufficient recombination of the *Gpr124^{CKO}* allele. Constitutive deletion of *Ndp* in the presence of one functional copy of *Gpr124* (upper panels) is associated with an intact BBB, sulfo-NHS-biotin leakage that is confined to the choroid plexus, and an absence of PLVAP in ECs. Constitutive deletion of *Ndp* combined with EC-specific deletion of *Gpr124* (lower panels) is associated with widely scattered BBB defects as shown by multiple zones of sulfo-NHS-biotin leakage in the cerebral cortex and hippocampus and by induction of PLVAP in a subset of ECs. The BBB is largely intact in the thalamus (white arrows). In (G) Coronal sections at the level of the colliculus/cerebellum junction show conversion of ECs from PLVAP-/claudin5+ to PLVAP+/claudin5- in the superior colliculus (top), cerebellum (center), and brainstem (bottom) with constitutive deletion of *Ndp* and postnatal EC-specific deletion of *Gpr124* (*Gpr124^{CKO/-};Ndp^{KO};Pdgfb-CreER*). Deletion of either gene alone shows little conversion. Mice were treated with 50-100 μ g 4HT at P3-P4, and brains were examined at P6. Scale bars: F, 500 μ m; G, 1 mm.

(H) Eliminating *Gpr124* in postnatal ECs has little or no effect on retinal vascular architecture or EC differentiation. Comparison of P6 retina flat mounts with the following number of functional *Gpr124* alleles in ECs following 50-100 μ g 4HT treatment at P3-P4: two (*Gpr124^{CKO/+}*), one (*Gpr124^{CKO/+};Pdgfb-CreER*), or zero (*Gpr124^{CKO/-};Pdgfb-CreER*). By contrast, a P6 *Ndp^{KO}* retina exhibits reduced vascular coverage, complete conversion of veins and capillaries from a PLVAP-/claudin5+ to a PLVAP+/claudin5- state, and partial conversion of arteries from a PLVAP-/claudin5+ to a PLVAP+/claudin5- state. Scale bar: 200 μ m.

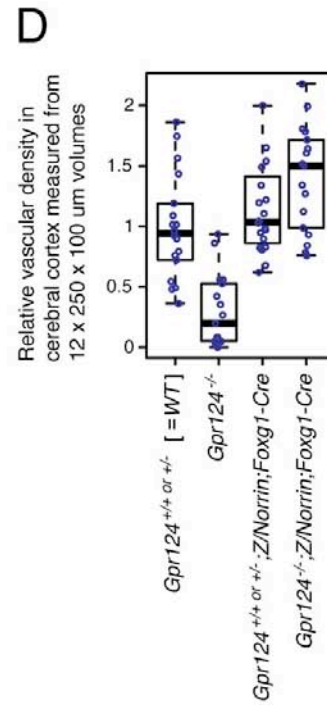
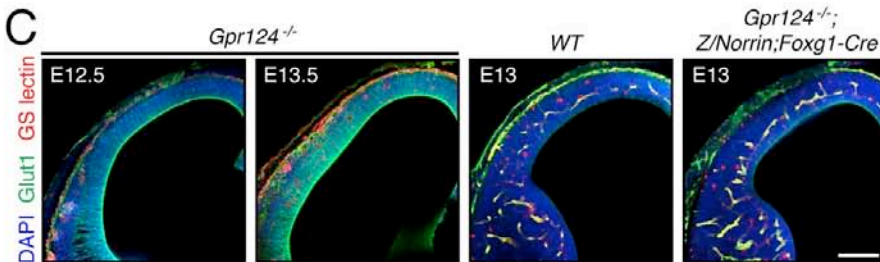
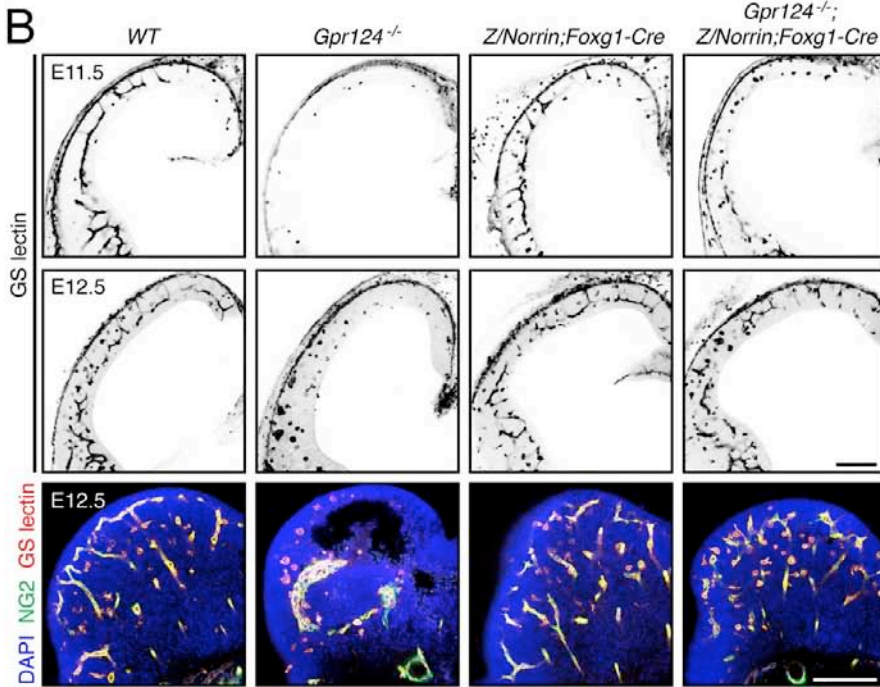
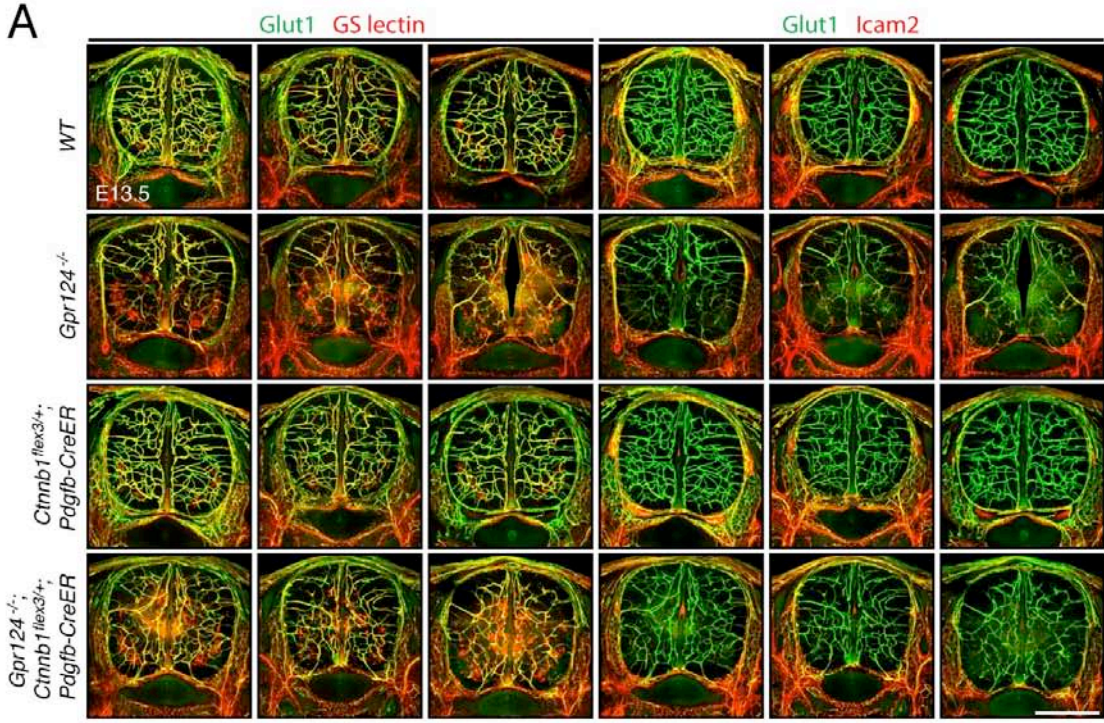


Figure S3, Related to Figure 4. Spinal cord vascularization defects in E13.5 *Gpr124*^{-/-} embryos are largely rescued by EC-specific stabilization of beta-catenin, and ectopic Norrin expression corrects the *Gpr124*^{-/-} angiogenesis phenotype in the cerebral cortex and MGE.

(A) For each genotype, sections at the forelimb level are shown from three E13.5 embryos treated at E10.5 with a maternal IP injection of 1.5 mg tamoxifen. The sections were stained for Glut1, Icam2, and GS lectin. Two of the three markers are shown in each image, with false coloring (red) of the channels for GS lectin (left) and Icam2 (right). The first and fourth columns derive from one section from the first embryo; the second and fifth columns derive from one section from the second embryo; and the third and sixth columns derive from one section from the third embryo. All *Gpr124*^{-/-} embryos exhibit a marked reduction in vascularization and reduced Glut1 expression in the ventral spinal cord, and both of these phenotypes are partially rescued in the *Gpr124*^{-/-}; *Ctnnb1*^{fl^{ex3}/+}; *Pdgfb-CreER* embryo three days after tamoxifen exposure. Scale bar: 500 μ m.

(B) Rescue of the *Gpr124*^{-/-} cerebral cortex angiogenesis defect at E11.5 and E12.5 by *Z/Norrin*; *Foxg1-Cre* (upper panels) and rescue of the MGE angiogenesis defect with restoration of normal vascular architecture and pericyte coverage (visualized with anti-NG2; lower panels).

(C) Rescue of the *Gpr124*^{-/-} cerebral cortex angiogenesis defect at E13 by *Z/Norrin*; *Foxg1-Cre*. Vascular architecture and Glut1 expression are restored. An age-matched *WT* control is shown together with *Gpr124*^{-/-} samples that are 0.5 days younger and 0.5 days older. The *Gpr124*^{-/-} phenotype remains constant during this time window. Scale bars: 200 μ m.

(D) Quantification of vascular density in the E13.5 cerebral cortex (based on GS lectin staining) shows a complete rescue of the *Gpr124*^{-/-} angiogenesis defect by *Z/Norrin*; *Foxg1-Cre*. We note that GS lectin stains both ECs and invading macrophages, and the automated procedure used to quantify vessel density (skeletonizing GS lectin+ objects in ImageJ) does not discriminate between the two. The result is an over-estimate of vascular density in the *Gpr124*^{-/-} cerebral cortex, i.e. an underestimate of the severity of the angiogenesis defect.

Supplemental Tables.

Table S1, Related to Figure 1. Abundance of transcripts coding for canonical Wnt signaling components in STF cells, determined by RNAseq.

Gene ID	Locus	FPKM	FPKM (low)	FPKM (high)
FZD1	chr7:90893782-90898131	4.16859	3.81319	4.31907
FZD10	chr12:130647031-130650284	0	0	0
FZD2	chr17:42634924-42636907	2.11461	1.73747	2.2608
FZD3	chr8:28351772-28421959	9.41438	8.67374	9.60003
FZD4	chr11:86656721-86666433	3.58846	3.37676	3.75492
FZD5	chr2:208627311-208634143	2.64747	2.46079	2.78816
FZD6	chr8:104310660-104345092	11.4404	11.067	11.9686
FZD7	chr2:202899309-202903160	8.31892	7.64247	8.47516
FZD8	chr10:35927176-35930362	5.56468	4.99341	5.66115
FZD9	chr7:72848108-72850449	1.47142	1.21908	1.62692
WNT1	chr12:49372235-49376395	0	0	0
WNT10A	chr2:219745254-219758651	0.00956023	0	0.0218478
WNT10B	chr12:49359123-49365641	1.21328	0.994821	1.3761
WNT11	chr11:75897370-75917574	6.50258	5.5283	6.48741
WNT16	chr7:120965420-120981157	0.0582791	0.0268792	0.0926115
WNT2	chr7:116916687-116963343	0.0499667	0.0193112	0.080715
WNT2B	chr1:113010039-113063908	0.52858	0.419277	0.638053
WNT3	chr17:44841686-44896082	2.13656	1.66487	2.31001
WNT3A	chr1:228194751-228248961	0.597247	0.484906	0.700813
WNT4	chr1:22443799-22469519	0.165807	0.124968	0.207394
WNT5A	chr3:55499743-55521331	2.2476	2.06949	2.40374
WNT5B	chr12:1726221-1756377	4.18774	3.8523	4.52318
WNT6	chr2:219724545-219738954	0.11099	0.0610453	0.158718
WNT7A	chr3:13860081-13921618	0.00687259	0	0.018164
WNT7B	chr22:46316247-46373008	1.20229	1.0505	1.33435
WNT8A	chr5:137419773-137427199	0.00801978	0	0.0207831
WNT8B	chr10:102222811-102243397	0.156534	0.0988848	0.213383
WNT9A	chr1:228109164-228135676	0.250424	0.142275	0.351503
WNT9B	chr17:44928967-44954437	0	0	0
LRP5	chr11:68080107-68216739	7.59131	7.09264	7.72454
LRP5L	chr22:25747385-25777544	3.08667	2.79324	3.39075
LRP6	chr12:12268962-12419811	7.40633	7.1144	7.63426
DVL1	chr1:1270658-1284492	18.4042	16.7186	18.0607
DVL2	chr17:7128660-7137863	13.8043	12.5282	13.6362
DVL3	chr3:183873283-183891313	5.87791	5.46874	6.06955
AXIN1	chr16:337439-402464	11.3651	10.9349	11.9157
AXIN2	chr17:63524684-63557740	4.30469	3.93273	4.45284
CTNNB1	chr3:41240941-41281939	155.755	156.429	160.094
APC	chr5:112043201-112181936	6.94088	6.77	7.21802
APC2	chr19:1450147-1473243	0.248305	0.216734	0.279097
LEF1	chr4:108968700-109090112	6.09404	5.55549	6.30067
TCF4	chr18:52889561-53255860	4.51687	4.35213	4.73148
WLS	chr1:68564142-68698284	37.3356	36.4227	38.7765

NDP	chrX:43808023-43832921	0	0	0
TSPAN12	chr7:120427375-120498177	11.2843	10.0536	11.1716

For each gene the values for fragments per kilobase of exon per million fragments mapped (FPKM) are listed in column 3, with low and high limits of the 95% confidence intervals for FPKM in columns 4 and 5, respectively.

Table S2, Related to Figures 2-4. Numbers of embryos analyzed for different genotypes shown in Figures 2-4.

Combinations of *Gpr124* and *Ndp* alleles at E11.5

Genotype	Number of embryos analyzed	
	Hindbrain	Spinal cord
<i>Gpr124</i> ^{+/+ or +/-} ; <i>Ndp</i> ^{WT or +/- or KO}	9	5
<i>Gpr124</i> ^{-/-} ; <i>Ndp</i> ^{WT}	8	4
<i>Gpr124</i> ^{-/-} ; <i>Ndp</i> ^{+/-}	2	2
<i>Gpr124</i> ^{-/-} ; <i>Ndp</i> ^{KO}	8	7

Combinations of *Gpr124* and *Fz4* alleles at E11.5

Genotype	Number of embryos analyzed
<i>Gpr124</i> ^{+/-} ; <i>Fz4</i> ^{-/-}	3
<i>Gpr124</i> ^{-/-} ; <i>Fz4</i> ^{+/-}	5

Combinations of *Gpr124*, *Ctnnb1*^{fl_{ex3}}, and *Pdgfb-CreER* alleles at E12.5-E13.5

Genotype	Number of embryos analyzed (by age)	
	E12.5	E13.5
<i>Gpr124</i> ^{+/- or +/+}	2	3
<i>Gpr124</i> ^{-/-}	0	3
<i>Gpr124</i> ^{+/- or +/+} ; <i>Ctnnb1</i> ^{fl_{ex3}/+} ; <i>Pdgfb-CreER</i>	0	3
<i>Gpr124</i> ^{-/-} ; <i>Ctnnb1</i> ^{fl_{ex3}/+} ; <i>Pdgfb-CreER</i>	1	4

Combinations of *Gpr124*, *Z/Norrin*, and *Foxg1-Cre* at E11.5-E13.5

Genotype	Number of embryos analyzed (by age)			
	E11.5	E12.5	E13	E13.5
<i>Gpr124</i> ^{+/- or +/+}	2	1	2	2
<i>Gpr124</i> ^{-/-}	1	2	0	3
<i>Gpr124</i> ^{+/- or +/+} ; <i>Z/Norrin</i> ; <i>Foxg1-Cre</i>	2	2	1	2
<i>Gpr124</i> ^{-/-} ; <i>Z/Norrin</i> ; <i>Foxg1-Cre</i>	2	1	1	2

Supplemental Experimental Procedures

Preparation and administration of 4HT and Tamoxifen

An ethanol:sunflower seed oil (Sigma-Aldrich) mixture (1:5 vol:vol) was added to solid 4HT (Sigma-Aldrich H7904) or tamoxifen (Sigma-Aldrich T5648) to achieve final concentrations of 4mg/ml or 50mg/ml, respectively. The sample was extensively shaken/vortexed at room temperature for 2-4 hours until completely dissolved, and stored in aliquots at -80°C. The thawed samples were vortexed and diluted as needed in sunflower seed oil prior to injection (final concentration ~1mg/ml for 4HT and 10-15mg/ml for tamoxifen). For pups, 50-100 µl 4HT was injected by the intraperitoneal (IP) route, and for pregnant females 100-150 µl tamoxifen was injected into the dorsal fat pad.

Tissue processing and immunohistochemistry

For postnatal brain vasculature, deeply anesthetized mice were perfused via an intra-cardiac route with 10-20 ml 0.3 mg/ml sulfo-NHS-LC-Biotin (Thermo Scientific 21335) in phosphate buffered saline (PBS), followed by ~20 ml 2% paraformaldehyde (PFA) in PBS. Dissected brains were post-fixed with 1% PFA for 3-4 hours, and then immersed in cold 100% methanol from 6 hours to overnight, followed by rehydration in PBS for 6 hours to overnight. For embryonic brain and spinal cord vasculature, embryos were fixed in 2-4% PFA overnight, and washed with PBS for 4-6 hours. Postnatal brains and embryos were embedded in 3% agarose, and 150 µm sections were cut on a vibratome. For retinal vasculature, mouse eyes were fixed in 2% PFA for 1-2 hours prior to dissection.

For immunostaining, sections and whole mount retinas were incubated overnight in primary antibodies diluted in PBSTC (PBS + 0.3% Triton + 0.1mM CaCl₂) + 10% normal goat serum, washed in PBSTC for 6-8 hours, and incubated overnight in secondary antibodies diluted in PBSTC + 10% normal goat serum (0.25% mouse serum was included as a competitive blocker when rat anti-PLVAP primary antibody was used). Sections and retinas were washed in PBSTC and flat-mounted in Fluoromount G (EM Sciences, 17984-25). All immersion-fixation, washing, and immunostaining steps were carried out at 4°C. Images were captured using a Zeiss LSM700 confocal microscope, and processed with ImageJ, Adobe Photoshop and Adobe Illustrator software.

Plasmids

The complete set of mouse Wnt and Frizzled expression plasmids are described in Yu et al. (2012). The mouse Gpr124 expression plasmid was a kind gift of Dr. Calvin Kuo (Stanford). The mouse Gpr125 expression plasmid was constructed by inserting the Gpr125 coding region (GE LifeSciences; accession BC052391) into pRK5; this cDNA sequence differs from the GenBank entry by an Ala30Pro substitution.

Luciferase assays

STF cells were plated in a 96-well plate at 15% to 30% confluence, and transfected with 150-200 ng plasmid DNA and 0.6 µl Fugene6 (Promega) per 3 wells. The DNA mix contained: 1 ng pRL-TK (Renilla luciferase internal control); 50 ng pRK5-NLS-GFP; 50 ng Gpr124, Tspan12, or control vector (pRK5) plasmids; 50 ng pRK5-Fz; 10 ng Wnt7a, Wnt7b, or Norrin plasmids (50 ng Wnts/Norrin were used in the screens of 19 Wnts and Norrin); and 5 ng Lrp plasmid, unless otherwise specified. Reporter activity was measured using the Dual-Luciferase Reporter Assay (Promega) with the standard protocol, and relative luciferase units (RLU) were calculated as Firefly/Renilla activity in each well. For Norrin stimulation, Norrin-AP conditioned medium was prepared as described in Smallwood et al., (2007) and incubated with transfected STF cells for 12-24 hours. For Wnt7a-HEK293 + STF cell co-culture, HEK293 and STF cells were plated separately in 12-well plate at 50% to 80% confluence, the 293 cells were transfected with 100 ng pRK5-NLS-GFP + 100 ng Wnt7a or pRK5 + 300 ng Gpr124 or pRK5 per well, and the STF cells were transfected with 3 ng pRL-TK + 150 ng pRK5-NLS-GFP + 150 ng Fz4 + 150 ng Gpr124 or pRK5 per well. 12-24 hours post-transfection, 293 cells and STF cells were dissociated with PBS, mixed at 1:1 ratio and plated in a 96-well plate at ~50% confluence, and grown for 24 to 30 hours before measuring luciferase activity.

Quantifications, boxplot and statistical analysis

For beta-galactosidase positive ECs in the MGE, 150 μm thick coronal sections of E11.5-E12.5 embryos were stained with anti-beta-galactosidase antibodies combined with GS lectin. For 1-2 sections per embryo, Z-stacked images encompassing $\sim 12 \mu\text{m}$ along the Z-axis were collapsed, and the beta-gal+ ECs in the vasculature over an area of $\sim 0.2 \text{ mm}^2$ (volume = 0.003 mm^3) within the MGE were counted.

For quantifying the avascular area in the spinal cord, 150 μm thick trunk cross sections of E11.5 embryos were stained with GS lectin. For 4-6 sections per embryo, Z-stacked images encompassing $\sim 21 \mu\text{m}$ along the Z-axis were collapsed, and total spinal cord area and avascular area were outlined and measured using ImageJ as indicated in Figure 2B.

For vascular invasion into the cerebral cortex, 150 μm thick coronal sections of E13.5 (for *Gpr124*^{-/-}; *Ctnnb1*^{fl^{ex3}/+}; *Pdgfb-CreER* experiments) and E13-E13.5 (for *Gpr124*^{-/-}; *Z/Norrin*; *Foxg1-Cre* experiments) embryos were stained with ICAM2. Z-stacked images encompassing 12 μm along the Z-axis were collapsed. For 4-8 sections per embryo, a 250 μm x 100 μm region within the cerebral cortex was cropped, thresholded, binarized, and skeletonized using imageJ with fixed sets of parameters for all images. The relative vascular lengths were measured by computing the pixel coverage (which is proportional to length) of the skeletonized vessels.

All box-plots were produced in RStudio with default settings. For statistical analysis, Fisher's exact test was performed for Table 1, and an unpaired two-tailed Student's t-test was performed for the boxplots.

Supplemental references

Smallwood, P.M., Williams, J., Xu, Q., Leahy, D.J., and Nathans, J. (2007). Mutational analysis of Norrin-Frizzled4 recognition. *J Biol Chem* 282, 4057-4068.

Yu, H.M., Ye, X., Guo, N., and Nathans, J. (2012). Frizzled 2 and frizzled 7 function redundantly in convergent extension and closure of the ventricular septum and palate: evidence for a network of interacting genes. *Development* 139, 4383-4394.